Proceedings of the International Symposium on Physics of Materials (ISPMA13)

# Determination of the Diffusion Coefficients of Boron in the FeB and $Fe_2B$ Layers Formed on AISI D2 Steel

M. Keddam[a,*], Z. Nait Abdellah[a,b], M. Kulka[c] and R. Chegroune[a]

[a]Laboratoire de Technologie des Matériaux, Département de Sciences des Matériaux, Faculté de Génie Mécanique et Génie des Procédés, USTHB, B.P. No. 32, 16111, El-Alia, Bab-Ezzouar, Algiers, Algeria

[b]Département de Chimie, Faculté des Sciences, Université Mouloud Mammeri, 15000 Tizi-Ouzou, Algeria

[c]Poznań University of Technology, Institute of Materials Science and Engineering, pl. M. Skłodowskiej-Curie 5, 60-965 Poznań, Poland

In the present work, a diffusion model was applied to estimate the boron diffusion coefficients in the FeB and $Fe_2B$ layers during the pack-boriding of AISI D2 steel in the temperature range of 1223–1323 K during a variable exposure time between 1 and 8 h. The mass balance equations were formulated at each growing interface by considering the effect of boride incubation times. The estimated values of boron activation energies in the FeB and $Fe_2B$ layers were compared with the literature data. Validation of the present model was made by comparing the experimental thickness of each boride layer, taken from the literature data, with the predicted values. In addition, a simple equation was suggested to estimate the required time to obtain a single $Fe_2B$ layer by diffusion annealing.

DOI: 10.12693/APhysPolA.128.740

PACS: 81.15.Aa, 68.55.A–,68.47.De, 68.55.jd

## 1. Introduction

Boriding (or boronizing) is a well-known thermochemical treatment in which boron is diffused into the surfaces of ferrous and non-ferrous alloys metal substrate to form a hard layer composed of metallic borides [1]. In particular, two kinds of iron borides (FeB and $Fe_2B$ having definite boron compositions [2]) can be formed at the surface of ferrous alloys (steels and Armco iron). As a consequence of this thermochemical treatment, properties such as wear resistance, surface hardness and corrosion resistance are improved. Boriding can be achieved with boron in different states such as solid powder, paste, liquid, gas and plasma. The widespread used method is pack-boriding (similar to pack-carburizing) because of its technical advantages [3, 4]. The pack contains a boron source such as a $B_4C$ compound, an activator to deposit atomic boron at the sample's surface and a diluent. The boriding process is realized in the temperature range of 1073–1273 K between 1 and 10 h. The morphology of the boride layers is influenced by the presence of alloying elements in the matrix. Saw-tooth-shaped layers are obtained in low-alloy steels whereas in high-alloy steels, the interfaces tend to be flat. The similar effect is visible depending on carbon content in the substrate. Carbon does not dissolve in FeB boride and its solubility in $Fe_2B$ boride is very low. Therefore, during boriding of steels, carbon is being moved in a core direction by following the boron diffusion front. Carbon is ejected from interstitial positions by boron, which forms iron borides at the surface. This phenomenon is accompanied by an increase in carbon concentration beneath iron borides, formed on the substrate of constant carbon content. Therefore, the high concentration of carbon makes difficult the boron diffusion. So, the iron borides produced on high-carbon steels show tendency towards a loss of the saw-tooth nature.

The modeling of the boriding kinetics is considered as a suitable tool to match the case depth with the intended industrial applications of the borided steel. Therefore, the modeling of the growth kinetics of boride layers has gained much attention to simulate the boriding kinetics during these last decades for the solid boriding [2, 4, 5–30] and recently for the gaseous boriding [31, 32].

In the present work, an original diffusion model [3] was suggested to estimate the boron diffusion coefficients in the FeB and $Fe_2B$ layers grown on AISI D2 steel including the effect of boride incubation times. A non-linear boron-concentration profile is assumed through the boride layers. The mass balance equations were applied to the two diffusion fronts: (FeB/$Fe_2B$) and ($Fe_2B$/substrate) interfaces in the temperature range of 1173–1323 K. In addition, a simple equation was proposed to estimate the required time to get a single $Fe_2B$ layer by diffusion annealing.

## 2. The mathematical model

The model considers the (FeB/$Fe_2B$) bilayer growth on the saturated substrate with boron atoms as displayed in Fig. 1. $C_{\text{up}}^{\text{FeB}}$ and $C_{\text{low}}^{\text{FeB}}$ (=16.23 wt%B) are the upper and lower boron concentrations in FeB while $C_{\text{up}}^{\text{Fe}_2\text{B}}$ (=9 wt%B) and $C_{\text{low}}^{\text{Fe}_2\text{B}}$ (=8.83 wt%B) are respectively the upper and lower boron concentrations in $Fe_2B$. $C_{\text{ads}}$ is the adsorbed concentration of boron [7]. $u$ is the position of the (FeB/$Fe_2B$) interface, $v$ is the position of the ($Fe_2B$/substrate) interface, $C_0$ is the boron solubility in

*corresponding author; e-mail: keddam@yahoo.fr

the matrix and equal to $35 \times 10^{-4}$ wt%B [8]. The upper boron content in the FeB phase ($C_{\text{up}}^{\text{FeB}}$), imposed by the boriding medium, gives rise to the two iron borides FeB and $Fe_2B$. From a thermodynamic point of view, the FeB phase exhibits a narrow composition range (of about 1 at.%B or 0.2 wt%B), as pointed out by Massalski [33]. The upper boron content in the FeB phase was taken in the composition range of (16.25–16.43 wt%B) to obtain a bilayer configuration consisting of the two iron borides FeB and $Fe_2B$.

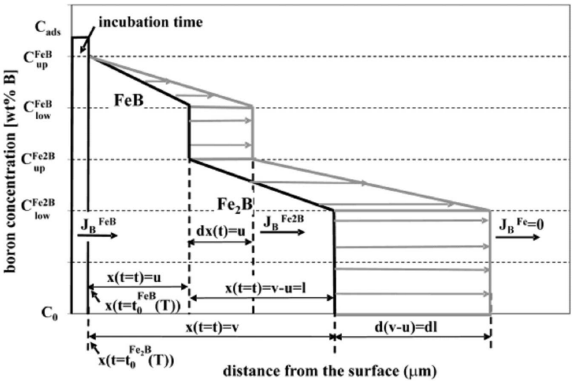


Fig. 1. Boron concentration profile through the FeB/$Fe_2B$ bilayer.

The following assumptions are taken into account during the establishment of the diffusion model:

- The kinetics is dominated by the diffusion-controlled mechanism;
- The growth of boride layers is a consequence of the boron diffusion perpendicular to the sample surface;
- The range of homogeneity of iron borides is about (1 at.%B) or (0.2 wt%B);
- The iron borides nucleate after a certain incubation time;
- The boride layer is thin in comparison with the sample thickness;
- Local equilibrium is occurred at the phase interfaces;
- Planar morphology is assumed for the phase interfaces;
- The volume change during the phase transformation is ignored;
- The diffusion coefficient of boron in each iron boride do not vary with the boron concentration and follows an Arrhenius relationship;
- A uniform temperature is assumed throughout the sample;
- No effect of the alloying elements on the boron diffusion is considered;
- The presence of porosity is ignored during the boron diffusion.

The initial conditions of the diffusion problem are set up as

$$C_{\text{FeB}}\{x(t>0)=0\}=0;\ C_{\text{Fe}_2\text{B}}\{x(t<0)=0\}=0;$$
$$C_{\text{Fe}}\{x(t<0)=0\}=0. \tag{1}$$

The boundary conditions are given by the following equations:

$$C_{\text{FeB}}\{\text{x(t}=\text{t}_0^{\text{FeB}}(\text{T}))=0\}=\text{C}_{\text{up}}^{\text{FeB}}$$
$$\text{for } C_{\text{ads}} < 16.23\text{wt.\% B}, \tag{2}$$

$$C_{\text{FeB}}\{\text{x(t}=\text{t}_0^{\text{FeB}}(\text{T}))=0\}=\text{C}_{\text{low}}^{\text{FeB}};$$
$$\text{for } C_{\text{ads}} \leq 16.23\text{wt.\% B and with FeB phase}, \tag{3}$$

$$C_{\text{Fe}_2\text{B}}\{x(t=t_0^{Fe_2B}(T))=0\}=C_{\text{up}}^{\text{Fe}_2\text{B}};$$
$$\text{for } 8.83\text{wt.\% B} \leq C_{\text{ads}} \prec 16.23\text{wt.\% B}$$
$$\text{and without FeB phase}, \tag{4}$$

$$C_{\text{Fe}_2\text{B}}\{x(t=t_0^{\text{Fe}_2\text{B}}(T))=0\}=C_{\text{low}}^{\text{Fe}_2\text{B}};$$
$$\text{for } C_{\text{ads}} \leq 8.83\text{wt.\% B and without FeB phase}, \tag{5}$$

$$C_{\text{FeB}}(x(t=t)=u)=C_{\text{low}}^{\text{FeB}}, \tag{6}$$

$$C_{\text{Fe}_2\text{B}}(x(t=t)=u)=C_{\text{up}}^{\text{Fe}_2\text{B}}, \tag{7}$$

$$C_{\text{Fe}_2\text{B}}(x(t=t)=v)=C_{\text{low}}^{\text{Fe}_2\text{B}}, \tag{8}$$

$$C_{\text{Fe}}(x(t=t)=v)=C_0. \tag{9}$$

The mass balance equations are given by Eqs. (10) and (11):

$$w_{\text{FeB}}\left(\frac{\text{d}u}{\text{d}t}\right)=[J_{\text{B}}^{\text{FeB}}-J_{\text{B}}^{\text{Fe}_2\text{B}}]_{x=u}, \tag{10}$$

$$w_{\text{Fe}_2\text{B}}\left(\frac{\text{d}v}{\text{d}t}\right)+w'\left(\frac{\text{d}u}{\text{d}t}\right)=[J_{\text{B}}^{\text{Fe}_2\text{B}}]_{x=v}, \tag{11}$$

with

$$w_{\text{FeB}}=[0.5\times(C_{\text{up}}^{\text{FeB}}-C_{\text{low}}^{\text{FeB}})+(C_{\text{low}}^{\text{FeB}}-C_{\text{up}}^{\text{Fe}_2\text{B}})];$$
$$w_{\text{Fe}_2\text{B}}=[0.5\times(C_{\text{up}}^{\text{Fe}_2\text{B}}-C_{\text{low}}^{\text{Fe}_2\text{B}})+(C_{\text{low}}^{\text{Fe}_2\text{B}}-C_0)];$$
$$w'=0.5\times(C_{\text{up}}^{\text{Fe}_2\text{B}}-C_{\text{low}}^{\text{Fe}_2\text{B}}).$$

The boron flux through a given boride layer is obtained from the Fick first law as follows:

$$J_{\mathrm{B}}^{i} = -D_{\mathrm{B}}^{i}\frac{\partial C_i(x,t)}{\partial x} \text{ with } i = (\mathrm{FeB} \text{ or } \mathrm{Fe_2B}) \quad (12)$$

$D_{\mathrm{B}}^{\mathrm{FeB}}$ and $D_{\mathrm{B}}^{\mathrm{Fe_2B}}$ are the diffusion coefficients of boron in the FeB and $Fe_2B$ layers, respectively. The distribution of boron concentration through the FeB layer is given by

$$C_{\mathrm{FeB}}(x,t) = C_{\mathrm{up}}^{\mathrm{FeB}} + \frac{C_{\mathrm{low}}^{\mathrm{FeB}} - C_{\mathrm{up}}^{\mathrm{FeB}}}{\mathrm{erf}\left(\frac{u}{2\sqrt{D_{\mathrm{B}}^{\mathrm{FeB}}t}}\right)} \times \mathrm{erf}\left(\frac{x}{2\sqrt{D_{\mathrm{B}}^{\mathrm{FeB}}t}}\right) \text{ for } 0 \le x \le u. \quad (13)$$

By the same way, the distribution of boron concentration through the $Fe_2B$ layer can be obtained as follows:

$$C_{\mathrm{Fe_2B}}(x,t) = C_{\mathrm{up}}^{\mathrm{Fe_2B}} + \frac{C_{\mathrm{low}}^{\mathrm{Fe_2B}} - C_{\mathrm{up}}^{\mathrm{Fe_2B}}}{\mathrm{erf}\left(\frac{u}{2\sqrt{D_{\mathrm{B}}^{\mathrm{Fe_2B}}t}}\right) - \mathrm{erf}\left(\frac{v}{2\sqrt{D_{\mathrm{B}}^{\mathrm{Fe_2B}}t}}\right)} \times \left[\mathrm{erf}\left(\frac{u}{2\sqrt{D_{\mathrm{B}}^{\mathrm{Fe_2B}}t}}\right) - \mathrm{erf}\left(\frac{x}{2\sqrt{D_{\mathrm{B}}^{\mathrm{Fe_2B}}t}}\right)\right] \text{ for u} \le \text{x} \le \text{v}. \quad (14)$$

The FeB layer thickness $u$ grows parabolically according to Eq. (15), where $k_{\mathrm{FeB}}$ represents the parabolic growth constant at the (FeB/$Fe_2B$) interface

$$u = k_{\mathrm{FeB}}(t - t_0^{\mathrm{FeB}}(T))^{1/2}. \quad (15)$$

The distance, $v$, is the location of the ($Fe_2B$/substrate) interface and $k$ the corresponding parabolic growth constant (Eq. (16)) and the difference ($l = v - u$) represents the $Fe_2B$ layer thickness given by Eq. (17):

$$v = k(t - t_0(T))^{1/2}, \quad (16)$$

$$l = v - u = k(t - t_0(T))^{1/2} - k_{\mathrm{FeB}}(t - t_0^{\mathrm{FeB}}(T))^{1/2}, \quad (17)$$

with $t_0^{\mathrm{FeB}}(T) < t_0(T)$ and $k < k_{\mathrm{FeB}}$, where $t_0(T)$ is the boride incubation time of the total boride layer (FeB+$Fe_2B$) and $t_0^{\mathrm{FeB}}(T)$ is the boride incubation time of FeB layer. The two temperature-dependent parameters $\beta_{\mathrm{FeB}}(T)$ and $\beta(T)$ are respectively given by Eqs. (18) and (19):

$$\beta_{\mathrm{FeB}}(T) = \left(1 - \frac{t_0^{\mathrm{FeB}}(T)}{t}\right)^{1/2} \quad (18)$$

and

$$\beta(T) = \left(1 - \frac{t_0(T)}{t}\right)^{1/2}. \quad (19)$$

The FeB layer thickness ($u$) is related to the $\beta_{\mathrm{FeB}}(T)$ parameter by Eq. (20):

$$u = k_{\mathrm{FeB}}\beta_{\mathrm{FeB}}(T)\sqrt{t}. \quad (20)$$

By the same way, the total layer thickness (FeB+$Fe_2B$) ($v$) is expressed by Eq. (21):

$$v = k\beta(T)\sqrt{t}. \quad (21)$$

## 3. Determination of boron diffusion coefficients in the FeB and $Fe_2B$ layers

To determine the boron diffusion coefficients in the FeB and $Fe_2B$ layers grown on AISI D2 steel, the experimental results taken from the M.Sc. thesis of Chavez-Gutiérrez [34] on the borided AISI D2 steel were used to validate the diffusion model. In this reference work, the powder-pack boriding was carried out at four temperatures (1173, 1223, 1273, and 1323 K) for three exposure times 4, 6 and 8 h using $B_4C$ Durborid as a boriding medium. Eighty measurements were performed on different cross-sections of the borided samples from the AISI D2 steel to determine the thickness of each boride layer. Tables I, II provide the experimental parabolic growth constants at each phase interface with the corresponding incubation times. The experimental values of parabolic growth constants at each phase interface were obtained from the slopes of the curves relating the squared boride layer thickness to the boriding time. The boride incubation times were deduced for a null boride layer thickness. It was shown that the higher boriding temperatures involve the shorter incubation times [22, 27] as shown in Tables I and II.

TABLE I

Experimental values of the parabolic growth constants $k_{\mathrm{FeB}}$ at the FeB/$Fe_2B$ interface in the temperature range of 1173–1323 K with the corresponding boride incubation times $t_0^{\mathrm{FeB}}(T)$.

| T [K] | $k_{\mathrm{FeB}}$ [$\mu$ms$^{-1/2}$] | $t_0^{\mathrm{FeB}}(T)$ [s] |
|---|---|---|
| 1223 | 0.176 | 1534.8 |
| 1253 | 0.201 | 1481.7 |
| 1273 | 0.276 | 1418.8 |
| 1323 | 0.355 | 1016.2 |

TABLE II

Experimental values of the parabolic growth constants $k$ at the $Fe_2B$/substrate interface in the temperature range of 1173–1323 K with the corresponding boride incubation times $t_0(T)$.

| T [K] | $k$ [$\mu$ms$^{-1/2}$] | $t_0(T)$ [s] |
|---|---|---|
| 1173 | 0.387 | 993.8 |
| 1223 | 0.445 | 593.3 |
| 1273 | 0.583 | 495.5 |
| 1323 | 0.751 | 419.3 |

TABLE III

Determination of the boron diffusion coefficients in [m$^2$s$^{-1}\times10^{-12}$] in each boride layer for an upper boron content of 16.40 wt% in the FeB layer.

| $T$ [K] | $D_{\mathrm{B}}^{\mathrm{FeB}}$ | $D_{\mathrm{B}}^{\mathrm{Fe_2B}}$ |
|---|---|---|
| 1223 | 2.48 | 2.17 |
| 1253 | 3.26 | 2.98 |
| 1273 | 5.91 | 4.79 |
| 1323 | 9.84 | 7.95 |

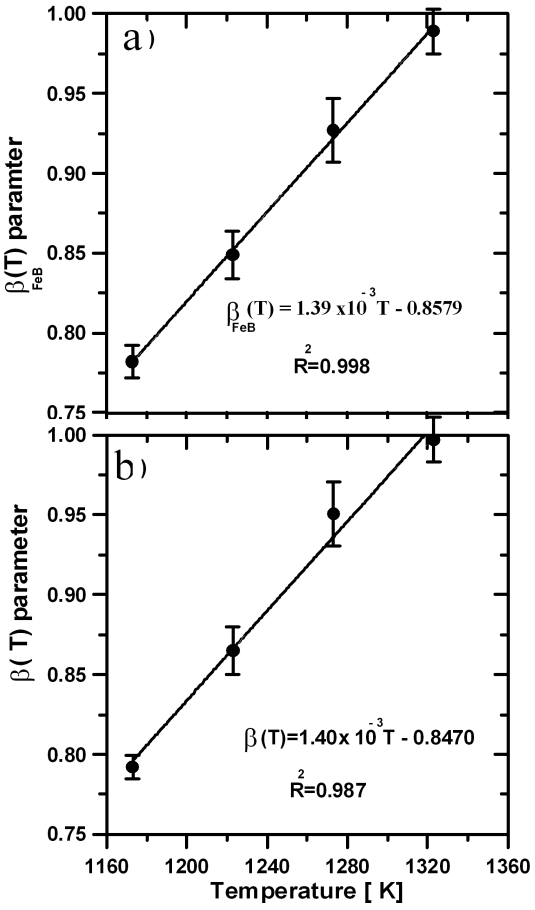


Fig. 2. Temperature dependence of the two parameters: (A) $\beta_{\mathrm{FeB}}(T)$ and (B) $\beta(T)$.

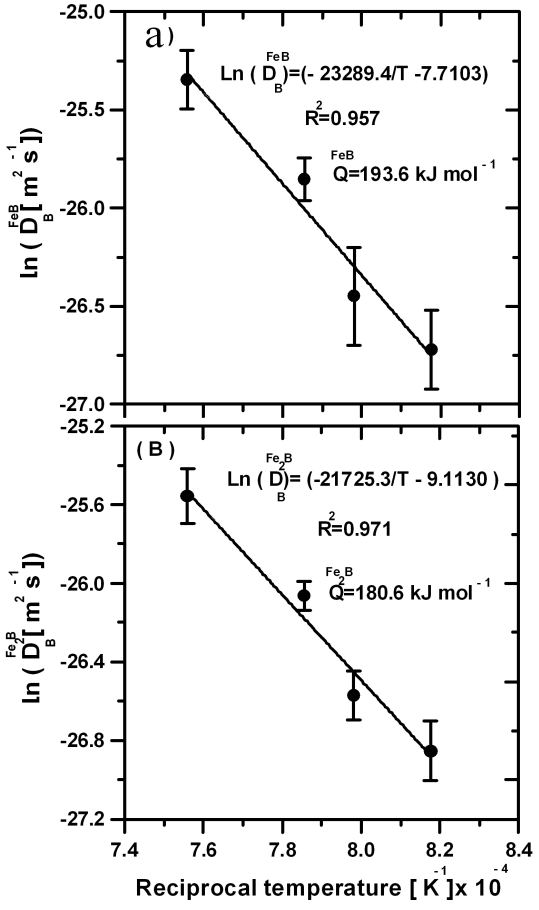


Fig. 3. Temperature dependence of the boron diffusion coefficient in each boride layer: (A) FeB layer, (B) $Fe_2B$ layer.

Figure 2 describes the temperature dependence of the two parameters $\beta_{\mathrm{FeB}}(T)$ and $\beta(T)$. It is noticed that these two parameters are linearly dependent on the boriding temperature and can be approximated by Eqs. (22) and (23) using a linear fitting of experimental data taken from Ref. [34]:

$$\beta_{\mathrm{FeB}}(T) = (1.39 \times 10^{-3} T - 0.8579) \tag{22}$$

and

$$\beta(T) = 1.40 \times 10^{-3} T - 0.8470. \tag{23}$$

For this purpose, a computer code written in Matlab (version 6.5) was used to estimate the boron diffusion coefficient in each boride layer. This program requires the following input data: (the time, the temperature, the lower and upper boron concentrations at each phase interface as well as the two parameters $\beta_{\mathrm{FeB}}(T)$ and $\beta(T)$). By solving the mass balance equations (Eqs. (10) and (11)) via the Newton–Raphson method [35], it is possible to determine the boron diffusion coefficients in the FeB and $Fe_2B$ layers. Table III summarizes the estimated values of boron diffusion coefficients in the FeB and $Fe_2B$ layers for an upper boron content equal to 16.40 wt% in the FeB phase.

TABLE IV

Values of boron activation energies in [kJ mol$^{-1}$] obtained for different borided steels. PP — powder-pack

| Material | Method | FeB | $Fe_2B$ | Ref. |
|---|---|---|---|---|
| AISI M2 | Paste | 283 | 239.4 | [36] |
| AISI4140 | Paste | – | 168.5 | [29] |
| AISI H13 | PP | – | 186.2 | [37] |
| AISI 316L | PP | 204 | 198 | [22] |
| AISI M2 | PP | 223 | 207 | [27] |
| AISI M2 | PP | 220.2 | 213 | [31] |
| AISI D2 | PP | 194 | 182 | [34] |
| AISI D2 | PP | 193.6 | 180.6 | this work |

Figure 3 gives the temperature dependence of boron diffusion coefficients in the FeB and $Fe_2B$ layers following the Arrhenius equation. The value of boron activation energy in each boride layer can be easily obtained from the slopes of the corresponding curves. Therefore, the boron diffusion coefficients in the FeB and $Fe_2B$ layers are respectively given by Eqs. (24) and (25):

TABLE V

Experimental (exp.) and simulated (Eq. number) values of the FeB and FeB+$Fe_2B$ layers thicknesses [µm] in the temperature $T$ of 1173–1323 K for different treatment times $t$ [h] with an upper boron content equal to 16.40 wt% in the FeB phase.

| $T$ | $t$ | FeB | | FeB+$Fe_2B$ | |
|---|---|---|---|---|---|
| | | exp. | (26) | exp. | (27) |
| 1223 | 1 | 10.68±2.7 | 8.90 | 24.11±2.6 | 19.90 |
| | 3 | 17.924±4.4 | 15.43 | 38.26±5.2 | 34.47 |
| | 5 | 24.01±3.2 | 19.92 | 46.09±5.9 | 44.50 |
| | 7 | 27.96±5.1 | 23.57 | 54.47±5.6 | 52.65 |
| 1253 | 1 | 14.19±3.9 | 11 .79 | 29.8±3.9 | 25.95 |
| | 3 | 23.76±5.6 | 20.42 | 46.69±6.0 | 44.95 |
| | 5 | 28.98±7.2 | 26.37 | 60.45±7.9 | 58.04 |
| | 7 | 32.76±6.1 | 31.20 | 69.99±7.2 | 68.87 |
| 1273 | 1 | 18.54±3.6 | 14.11 | 40.19±5.9 | 30.77 |
| | 3 | 25.92±5.2 | 24.44 | 53.23±6.3 | 53.30 |
| | 5 | 29.02±7.6 | 31.55 | 77.57±8.6 | 68.81 |
| | 7 | 35.11±6.7 | 37.34 | 84.13±11.2 | 81.41 |
| 1323 | 1 | 26.04±6.0 | 21.59 | 55.58±7.4 | 46.06 |
| | 3 | 31.64±8.3 | 37.39 | 79.39±9.7 | 79.77 |
| | 5 | 35.24±8.8 | 48.27 | 93.46±11.8 | 102.99 |
| | 7 | 39.97±9.9 | 57.12 | 105.88±13.1 | 121.86 |

TABLE VI

Estimation of the $Fe_2B$ layer thickness after diffusion annealing (Eq.(30); in [µm]) and the annealing time $t_{u_{\mathrm{FeB}}} = 0$ (Eq. (28)) required to eliminate the FeB layer for the borided samples at different temperatures $T$ for 7 h (Eq. (28)). $P$ — FeB, $Q$ — $Fe_2B$, $R$ — $Fe_2B$ after diffusion annealing, Eq.(30); in [µm].

| $T$ [K] | $P$ | $Q$ | $R$ | $t_{u_{\mathrm{FeB}=0}}$ [h] |
|---|---|---|---|---|
| 1223 | 23.57 | 52.65 | 95.55 | 6.89 |
| 1253 | 31.20 | 68.67 | 125.46 | 7.78 |
| 1273 | 37.34 | 81.41 | 149.38 | 8.40 |
| 1323 | 57.12 | 121.86 | 225.84 | 10.10 |

$$D_{\mathrm{B}}^{\mathrm{FeB}} = 4.48 \times 10^{-4} \times \exp\left(\frac{-193.6\ \mathrm{kJ/mol}}{RT}\right)\ \mathrm{m^2/s}, \quad (24)$$

$$D_{\mathrm{B}}^{\mathrm{Fe_2B}} = 1.10 \times 10^{-4} \times \exp\left(\frac{-180.6\ \mathrm{kJ/mol}}{RT}\right)\ \mathrm{m^2/s}, \quad (25)$$

where $R$ is the universal gas constant (= 8.314 J/(mol K)), and $T$ represents the absolute temperature in K. The reported values of the activation energies [22, 27, 29, 30, 34, 36, 37] of the borided steels are listed in Table IV together with the values from this work. The obtained values of the activation energies are found to be dependent on the boriding method and on the chemical composition of the substrates. Assuming that the parabolic growth constants $k_{\mathrm{FeB}}$ and $k$ obey the Arrhenius equation, Eqs. (20) and (21) can be rewritten as follows:

$$u = 1.8 \times 10^4 \exp(-\frac{14320.1}{T})\sqrt{t}, \quad (26)$$

$$v = 2 \cdot 2 \times 10^4 \exp(-\frac{13578.3}{T})\sqrt{t}, \quad (27)$$

where $T$ is the boriding temperature in K, $u$ and $v$ are given in $\mu$m.

In Table V, the predicted values of the boride layers thicknesses are compared with the experimentally determined values in the temperature range of 1173–1323 K for a treatment time varying from 80 to 240 min. A good concordance was then observed between the experimental data and the simulation results for an upper boron content equal to 16.40 wt% in the FeB phase.

## 4. Total elimination of the FeB layer by diffusion annealing

In industrial practice, it is possible to reduce the brittleness of boride layers by controlling their microstructural nature. It is known that a single $Fe_2B$ boride layer is more desirable than a dual FeB–$Fe_2B$ layer [38]. It makes possible to reduce the FeB layer thickness by applying a diffusion annealing in $H_2$ atmosphere. During this stage, the supply of boron is stopped since the concentration gradient of boron in FeB is null (i.e. $C_{\mathrm{up}}^{\mathrm{FeB}} = C_{\mathrm{low}}^{\mathrm{FeB}} = 16.23$ wt%B), the FeB layer will be converted into $Fe_2B$ layer. The time required to eliminate the FeB layer during the diffusion annealing can be obtained from Eq. (28):

$$t_{u_{\mathrm{FeB}=0}} = \frac{u \times l \times \left(C_{\mathrm{low}}^{\mathrm{FeB}} - C_{\mathrm{up}}^{\mathrm{Fe_2B}}\right)}{D_{\mathrm{B}}^{\mathrm{Fe_2B}}\left(C_{\mathrm{up}}^{\mathrm{Fe_2B}} - C_{\mathrm{low}}^{\mathrm{Fe_2B}}\right)}, \quad (28)$$

where $u$ is the FeB layer thickness ($\mu$m), $l$ is the $Fe_2B$ boride thickness ($\mu$m) and $D_{\mathrm{B}}^{\mathrm{Fe_2B}}$ represents the boron diffusion coefficient in $Fe_2B$. It is seen that the annealing time depends on the boron diffusion coefficient in $Fe_2B$, and also on the thickness of each boride layer. During the diffusion annealing, infinitesimal reduction of FeB layer is related to the infinitesimal growth of $Fe_2B$ layer by Eq. (29):

$$\Delta u = -\left(\frac{w_{\mathrm{Fe_2B}}}{w_{\mathrm{FeB}} + w_{\mathrm{Fe_2B}} + w'}\right)\Delta l = -0.5493\Delta l. \quad (29)$$

The value of $Fe_2B$ layer thickness $l'$ (in $\mu$m) after diffusion annealing becomes

$$l' = l + \frac{\Delta u}{0.5493}. \quad (30)$$

Table VI gathers the simulation results obtained from Eqs. (28) and (30) to estimate the $Fe_2B$ layer thickness after diffusion annealing and the time required to eliminate the FeB layer in case of the borided samples treated at different temperatures for 10 h of treatment. The obtained annealing times are increased with an increase of boriding temperature since the boride layer becomes thicker. In this context, Kulka et al. [31] have experimentally determined the annealing time using $H_2$ atmosphere to get a single $Fe_2B$ layer on the gas borided Armco Fe at 1173 K for 2 h in a gas mixture ($H_2$–$BCl_3$). They

found that the total elimination of FeB layer was after about 1 h. The diffusion annealing of previously pack-borided AISI 1045 steel was also studied by Campos-Silva et al. [39]. Boronizing parameters were as follows: 1223 K and 8 h. The annealing process, carried out at 1273 K for 8 h, caused that FeB phase disappeared completely. Furthermore, it was shown by Dybkov et al. [40] that annealing of a borided Fe–Cr sample for 6 h also resulted in the disappearance of FeB layer.

## 5. Conclusion

In the present work, an original diffusion model was suggested to estimate the boron diffusion coefficients in the FeB and $Fe_2B$ layers grown on AISI D2 steel. The derived mass balance equations at the (FeB/$Fe_2B$) and ($Fe_2B$/substrate) interfaces were used for obtaining the boron activation energies in the FeB and $Fe_2B$ layers. The values of boron activation energies for the AISI D2 steel were 193.6 and 180.6 kJ mol$^{-1}$ for the FeB and $Fe_2B$ layers, respectively. In addition, an approach was also proposed to estimate the required time to eliminate the FeB layer for the given boriding conditions. It is concluded that the formation of a single $Fe_2B$ layer on AISI D2 steel depended on the boriding parameters.

## References


[1] A.K. Sinha, *J. Heat Treat.* **4**, 437 (1991).

[2] C.M. Brakman, A.W.J. Gommers, E.J. Mittemeijer, *J. Mater. Res.* **4**, 1354 (1989).

[3] C. Meric, S. Sahin, S.S. Yilmaz, *Mater. Res. Bull.* **35**, 2165 (2000).

[4] M. Keddam, S.M. Chentouf, *Appl. Surf. Sci.* **252**, 393 (2005).

[5] D.S. Kukharev, S.P. Fizenko , S.I. Shabunya, *J. Eng. Phys. Therm.* **69**, 187 (1996).

[6] M. Keddam, *Appl. Surf. Sci.* **236**, 451 (2004).

[7] L.G. Yu, X.J. Chen, K.A. Khor, G. Sundararajan, *Acta Mater.* **53**, 2361 (2005).

[8] M. Keddam, *Appl. Surf. Sci.* **253**, 757 (2006).

[9] I. Campos, M. Islas, G. Ramírez, L. Zuniga, C. VillaVelázquez, C. Mota, *Appl. Surf. Sci.* **253**, 6226 (2007).

[10] I. Campos, G. Ramírez, U. Figueroa, C.V. Velázquez, *Surf. Eng.* **23**, 216 (2007).

[11] I. Campos-Silva, M. Ortiz-Domínguez, C. Villa-Velazquez, R. Escobar, N. López, *Defect Diffus. Forum* **272**, 79 (2007).

[12] I. Campos, G. Ramírez, U. Figueroa, J. Martinez, O. Morales, *Appl. Surf. Sci.* **253**, 3469 (2007).

[13] R.D. Ramdan, T. Takaki, Y. Tomita, *Mater. Trans.* **49**, 2625 (2008).

[14] M. Keddam, *Defect Diffus. Forum* **273-276**, 318 (2008).

[15] I. Campos-Silva, M. Ortiz-Dominguez, N. Lopez-Perrusquia, R. Escobar-Galindo, O.A. Gomez-Vargas, E. Hernandez-Sanchez, *Defect Diffus. Forum* **283-286**, 681 (2008).

[16] M. Keddam, *Int. J. Mater. Res.* **100**, 901 (2009).

[17] I. Campos-Silva, M. Ortiz-Domínguez, M. Keddam, N. López-Perrusquia, A. Carmona-Vargas, M. Elias-Espinosa, *Appl. Surf. Sci.* **255**, 9290 (2009).

[18] I. Campos-Silva, N. López-Perrusquia, M. Ortiz-Domínguez, U. Figueroa-López, O.A. Gómes-Vargas, A. Meneses-Amador, G. Rodríguez-Castro, *Kovove Mater.* **47**, 1 (2009)(in Russian).

[19] I. Campos-Silva, M. Ortíz-Domínguez, *Int. J. Microstruct. Mater. Prop.* **5**, 26 (2010).

[20] M. Ortiz-Domínguez, E. Hernandez-Sanchez, J. Martinez-Trinídad, M. Keddam, I. Campos-Silva, *Kovove Mater.* **48**, 1 (2010).

[21] M. Keddam, R. Chegroune, *Appl. Surf. Sci.* **256**, 5025 (2010).

[22] I. Campos-Silva, M. Ortiz-Domínguez, O. Bravo-Bárcenas, M.A. Doñu-Ruiz, D. Bravo-Bárcenas, C. Tapia-Quintero, M.Y. Jiménez-Reyes, *Surf. Coat. Technol.* **205**, 403 (2010).

[23] M. Keddam, M. Ortiz-Domínguez, I. Campos-Silva, J. Martinez-Trinídad, *J. Appl. Surf. Sci.* **256**, 3128 (2010).

[24] M. Keddam, *Defect Diffus. Forum* **297-301**, 269 (2010).

[25] M. Ortiz-Dominguez, I. Campos-Silva, J. Martinez-Trinidad, M. Elias-Espinosa, E. Hernandez-Sanchez, D. Bravo-Barcenas, *Defect Diffus. Forum* **297-301**, 294 (2010).

[26] M. Keddam, *Appl. Surf. Sci.* **257**, 2004 (2011).

[27] I. Campos-Silva, M. Ortiz-Domínguez, C. Tapia-Quintero, G. Rodríguez-Castro, M.Y. Jiménez-Reyes, E. Chávez-Gutiérrez, *J. Mater. Eng. Perform.* **21**, 1714 (2012).

[28] Z. Nait Abdellah, M. Keddam, A. Elias, *Acta Phys. Pol. A* **122**, 588 (2012).

[29] Z. Nait Abdellah, M. Keddam, A. Elias, *Int. J. Mater. Res.* **104**, 260 (2013).

[30] Z. Nait Abdellah, M. Keddam, *Mater. Technol.* **48**, 237 (2014).

[31] M. Kulka, N. Makuch, A. Pertek, L. Maldzinski, *J. Solid State Chem.* **199**, 196 (2013).

[32] M. Keddam, M. Kulka, N. Makuch, A. Pertek, L. Małdziński, *Appl. Surf. Sci.* **298**, 155 (2014).

[33] T.B. Massalski, *Binary Alloys Phase Diagrams*, 2nd ed., ASM International, Metals Park 1990.

[34] E. Chavez-Gutiérrez, M.Sc. Thesis, IPN, Mexico 2012 (in Spanish).

[35] W.H. Press, B.P. Flannery, S.A. Teukolsky, *Numerical Recipes in Pascal: The Art of Scientific Computing*, Cambridge University, 1989.

[36] I. Campos, R. Torres, O. Bautista, G. Ramirez, L. Zuniga, *Appl. Surf. Sci.* **252**, 2396 (2006).

[37] K. Genel, *Vacuum* **80**, 451 (2006).

[38] G. Celebi, M. Ipek, C. Bindal, A.H. Ucisik, *Mater. Forum* **29**, 456 (2005).

[39] I. Campos-Silva, M. Flores-Jiménez, G. Rodríguez-Castro, E. Hernández-Sánchez, J. Martínez-Trinidad, R. Tadeo-Rosas, *Surf. Coat. Technol.* **237**, 429 (2013).

[40] V.I. Dybkov, W. Lengauer, K. Barmak, *J. Alloys Comp.* **398**, 113 (2005).